

## Article

# Study of an Environmentally Friendly Method for the Dissolution of Precious Metal with Ionic Liquid and Iodoalkane

Feng Feng, Jiamei Liu, Mingxing Zhao, Lu Yu, Haixin Wang, Chunshan Lu, Qunfeng Zhang, Jia Zhao, Yanxia Sun \*, Jie Cen \* and Xiaonian Li \*

Institute of Industrial Catalysis, College of Chemical Engineering, Zhejiang University of Technology, Hangzhou 310014, China; ffeng@zjut.edu.cn (F.F.); jiameiliu@hotmail.com (J.L.); mingxingzhao0103@hotmail.com (M.Z.); yuluuni2014@gmail.com (L.Y.); 2112001484@zjut.edu.cn (H.W.); lcszjcn@zjut.edu.cn (C.L.); zhangqf@zjut.edu.cn (Q.Z.); jiazhao@zjut.edu.cn (J.Z.)

\* Correspondence: sunyanxia@zjut.edu.cn (Y.S.); jcen@zjut.edu.cn (J.C.); xnli@zjut.edu.cn (X.L.)

**Abstract:** Gold as a precious metal resource has high recycling significance. However, the current extraction methods cannot achieve the both efficiency and environmental friendliness. In this paper, we propose a new gold leaching agent, which can leach gold under light condition by mixing iodoform ( $\text{CHI}_3$ ) with 1-butyl-3-methylimidazolium dicyanamide ( $\text{BmimN}(\text{CN})_2$ ) ionic liquid. Under  $25\text{ }^\circ\text{C}$  and 13 W incandescent lamp irradiation, the leaching yield of gold can achieve 100 wt%, and the average leaching rate is 945 mg Au/(h·mol- $\text{CHI}_3$ ) (18.9 times of that of the cyanidation method). Through the analysis of the results of radical inhibition experiment, UV-Vis and XPS, a possible leaching mechanism is proposed: the iodine radical generated by light oxidizes  $\text{Au}^0$  to  $\text{Au}^+$ , and then forms  $\text{AuN}(\text{CN})_2$  by coordinating with  $\text{N}(\text{CN})_2^-$ . Subsequently, the ionic liquid and  $\text{AuN}(\text{CN})_2$  form a stable  $[\text{Bmim}][\text{AuN}(\text{CN})_2]$  ion pair structure, further promoting the dissolution reaction. The leaching yield of gold can reach 81.9 wt% and 100 wt%, respectively, when applied to ore and waste electrical and electronic equipment (WEEE); the leaching yield of gold can also reach 100 wt% when applied to a waste catalyst by adding a Soxhlet extraction. The results show that this method is not only efficient, mild, and environmentally friendly, but also has strong adaptability and wide application prospects.

**Keywords:** gold recovery; ionic liquid; free radical; waste catalyst; oxidation-complexation



**Citation:** Feng, F.; Liu, J.; Zhao, M.; Yu, L.; Wang, H.; Lu, C.; Zhang, Q.; Zhao, J.; Sun, Y.; Cen, J.; et al. Study of an Environmentally Friendly Method for the Dissolution of Precious Metal with Ionic Liquid and Iodoalkane.

*Metals* **2021**, *11*, 919. <https://doi.org/10.3390/met11060919>

Academic Editor: Yoshitsugu Kojima

Received: 16 April 2021

Accepted: 1 June 2021

Published: 4 June 2021

**Publisher's Note:** MDPI stays neutral with regard to jurisdictional claims in published maps and institutional affiliations.



**Copyright:** © 2021 by the authors. Licensee MDPI, Basel, Switzerland. This article is an open access article distributed under the terms and conditions of the Creative Commons Attribution (CC BY) license (<https://creativecommons.org/licenses/by/4.0/>).

## 1. Introduction

Gold as a precious metal can be used not only as currency but also in jewelry, in the pharmaceutical industry, and other fields [1,2]. The price of gold remains high and the demand has increased in recent years.

Due to its excellent conductivity and stability, gold plays an important role in electronic products; it is conducive to conductivity and shows oxidation resistance. Gold catalyst can be used in environmental catalysis (e.g., de- $\text{NO}_x$ , CO oxidation, photocatalysis, and catalytic combustion of volatile organic compounds (VOCs)), chemical synthesis (e.g., selective hydrogenation and oxidation, partial oxidation of  $\text{H}_2$  to form  $\text{H}_2\text{O}_2$ , and C-C coupling) and energy processing (e.g., the water-gas shift reaction, steam reforming of methane, and selective CO oxidation in excess  $\text{H}_2$ ) [3–10].

Leaching gold from ore is currently the main way to obtain gold. However, with the increasing demand for gold, ore resources are in short supply, and the ore is often of low grade, is difficult to concentrate, and contains many impurities. Generally, secondary resources (such as WEEE and spent catalysts) contain higher gold content than ore: ordinary gold mines usually have a grade of 0.3–17 g/t, while the gold content in mobile phone circuit boards is as high as 300–350 g/t [11]. Gold cannot be directly dissolved by ordinary acid and alkali due to its high electronegativity and high electrode potential.

At present, the most common extraction method in the metallurgical industry is the cyanidation method, which uses cyanide ion ( $\text{CN}^-$ ) to coordinate with gold to reduce its electrode potential to  $-0.64\text{ V}$ , so that a fast gold dissolution rate can be achieved. However, cyanide is toxic and harmful to the environment [12,13]. Other alternative methods using as thiourea, thiosulphate, and  $\text{KI}/\text{I}_2$  also cannot achieve both environmental friendliness and high efficiency [14–18]. Therefore, it is of great significance to develop a novel leaching method for gold.

Ionic liquids (ILs) have many outstanding advantages due to their unique structure and interaction, such as non-volatility, good thermal stability, reusability, and good extraction ability for various organic compounds and metal ions [19]. Electrostatic interaction is a common mechanism for the extraction of noble metal ions by ionic liquids. In addition, ionic liquids can form corresponding extended hydrogen bonds and have unique electronic and spatial interactions with noble metals making them the ideal candidate for metal extraction [20–22].

As a commonly used fungicide and preservative,  $\text{CHI}_3$  is non-allergenic, non-irritant, and has low toxicity. Moreover, iodoform can produce free radicals, which has strong oxidation under light condition.

Therefore, our study proposes a new gold leaching agent using  $\text{BmimN}(\text{CN})_2$  ionic liquid mixed with  $\text{CHI}_3$ , which can achieve high gold extraction yield from ore, WEEE, and spent catalyst under normal pressure, normal temperature, and light irradiation. This new agent is proved to have synthetic advantages and low environmental impact.

## 2. Materials and Methods

### 2.1. Materials

Gold powder,  $\text{CHI}_3$  at the purity of 99 wt%, chloroauric acid ( $\text{HAuCl}_4$ ), acetone ( $\text{CH}_3\text{COCH}_3$ ), and silica ( $\text{SiO}_2$ ) were provided by Aladdin (Shanghai Aladdin Biochemical Technology Co., Ltd, Shanghai, China).  $\text{BmimN}(\text{CN})_2$  at a purity of 99 wt% was obtained from the Lanzhou Institute of Physical Chemistry, Chinese Academy of Sciences. Gold ores were purchased from Suichang Gold Mine located in Suichang, Lishui, Zhejiang, China. CPU (Intel XEON™) was bought from Beijing Hongrong Century Technology Co., Ltd (Beijing, China).

### 2.2. Experimental Procedures

#### 2.2.1. Preparation of $\text{Au@SiO}_2$ Catalyst

$\text{Au@SiO}_2$  catalyst were prepared by impregnation method [23]. Ten grams of silica carrier was added into a 250 mL round bottomed flask containing 100 mL deionized water and stirred at  $80\text{ }^\circ\text{C}$  for 10 min at a speed of 200 r/min. Then, 10 mL of  $\text{HAuCl}_4$  solution with the concentration of 0.0193 g/mL was added dropwise to the obtained solution and continuously stirred for 4 h before adjusting the pH to 7 with NaOH solution. Ten milliliters of 80 wt%  $\text{N}_2\text{H}_4\cdot\text{H}_2\text{O}$  was later added into the flask, and stirred at  $40\text{ }^\circ\text{C}$  for another 30 min. After filtration, the filtrate was washed with deionized water until it was neutral and dried in a vacuum at  $110\text{ }^\circ\text{C}$  for 12 h.

#### 2.2.2. Preparation of Gold Ore Powder

Due to the large volume of the ore, and because part of the gold is covered by other minerals, the preparation methods of gold ore powder samples are as follows: 1. The large ore ( $25\text{ cm} \times 22\text{ cm} \times 14\text{ cm}$ ) was hammered into small pieces ( $<1\text{ cm} \times 1\text{ cm} \times 1\text{ cm}$ ). 2. Small pieces of ore were put into the grinding machine (model: FS400, brand: XFK, Fangke instrument (Changzhou) Co., Ltd., Jiangsu, China, power: 1650 W, speed: 28,000 r/min) to crush for 5 min. 3. The crushed ore powder was screened through a 400 mesh (0.00374 mm) screen, and then the ore powder smaller than 0.00374 mm was used in the experiment.

### 2.2.3. Preparation of CPU Pins

The main body of CPU pin is copper, and the surface is plated with gold. Therefore, the CPU pins (1.6 mm × φ0.3 mm) were directly cut off from the CPU by nipper pliers and used in the test.

### 2.2.4. Analysis of Metal Content in Ore Powder and Au@SiO<sub>2</sub> Catalyst

To accurately determine the leaching yield, it is necessary to analyze the original metal content in different samples. X-ray fluorescence (XRF) (Thermo Fisher Scientific, Waltham, MA, USA) can be used to directly measure the metal content of gold ore powder and Au@SiO<sub>2</sub> catalyst [24,25].

### 2.2.5. General Leaching Procedure by CHI<sub>3</sub>/BmimN(CN)<sub>2</sub>

Typically, the metal sources (except for Au@SiO<sub>2</sub> catalyst) were mixed with CHI<sub>3</sub>/BmimN(CN)<sub>2</sub> solution (CHI<sub>3</sub> = 0.5 g, BmimN(CN)<sub>2</sub> = 3 g) and stirred at a constant speed of 600 rpm for 5 h under the condition of 13 W incandescent lamp irradiation. The reactant solution was filtered by a 0.22 μm membrane and the concentration of gold or other metals of the solution was determined by atomic absorption spectrometry (AAS) (Beijing Puxi General Instruments Co., Ltd., Beijing, China). Finally, the leaching yield for each metal was calculated according to Equation (1).

$$\text{Leaching yield} = \frac{\text{Metal mass in solution}}{\text{Initial metal mass}} \times 100 \text{ wt\%} \quad (1)$$

### 2.2.6. Metal Leaching from Catalyst by CHI<sub>3</sub>/BmimN(CN)<sub>2</sub>

Due to the adsorption of catalyst support, the metal solution may remain in the pore and surface of the catalyst after leaching with CHI<sub>3</sub>/BmimN(CN)<sub>2</sub>. Thus, Soxhlet extraction was applied to the leached catalysts by CHI<sub>3</sub>/BmimN(CN)<sub>2</sub> using acetone as the solvent. The metal concentration in extracted solution and leaching solution was determined by AAS respectively. The leaching yield was calculated according to Equation (1).

## 2.3. Characterization and Method

X-ray fluorescence (XRF) measurements were performed on ARLADVANT'S X-4200 X-ray fluorescence spectrometer (Thermo Fisher Scientific, Waltham, MA, USA). The samples were dried at 105 °C for more than 2 h and then pressed into circular discs by a tablet press machine. Finally, the data were analyzed by software UNIQANT (20 May 2020).

X-ray diffraction (XRD) patterns were measured by an X'Pert PRO X-ray diffractometer (PANalytical B.V., Almelo, Netherlands) using a Cu-K $\alpha$  radiation with an X-ray source ( $\lambda = 0.154056$  nm) at 40 kV.

Single crystal X-ray diffraction (SXRD) was acquired by Smart Apex II DUO single crystal X-ray diffractometer (Bruker Corporation, Karlsruhe, Germany). The monochromatic Mo-K $\alpha$  ray ( $\lambda = 0.7107$  Å) of graphite monochromator was used as the incident light source (Bruker Corporation, Karlsruhe, Germany). The diffraction intensity was corrected by LP factor and SORTAV absorption, and the data processing was completed by SAINT program (Bruker Corporation, Karlsruhe, Germany).

X-ray photoelectron spectra (XPS) were acquired with a Kratos AXIS Ultra DLD spectrometer (KRATOS, Manchester, Britain). XPS analysis was performed with the monochromatic Al-K $\alpha$  as the excitation source (KRATOS, Manchester, Britain), in which the working voltage was 15 kV, and the emission current was 3 mA. As the ionic liquid is liquid at room temperature, the obtained ionic liquid solution was tested by XPS with filter paper as a support. The samples were made as follows: 1. The ionic liquid solution was dropped on the filter paper. 2. The filter paper was placed under the infrared lamp for 2–4 h until it was completely dried. 3. The filter paper adsorbed the ionic liquid solution and was cut into small pieces (4 mm × 6 mm) and glued on the glass slide (4 mm × 6 mm) with double-sided adhesive tape. 4. The sample was vacuumized overnight (>12 h) in the first

vacuum chamber of the instrument. The vacuum during the test was  $10^{-6}$  Pa. All XPS spectra were corrected C1s with standard binding energy of 284.8 eV.

Ultraviolet-visible spectrophotometry (UV-Vis) was performed on Cary-100 Ultraviolet-visible spectrophotometer (VARIAN, Palo Alto, CA, USA) at room temperature. With isopropanol as reference, the absorption spectrum of the sample in the range of 200–800 nm was determined after the background of the solvent was removed.

AAS results were obtained by air-acetylene flame method of TAS-990 atomic absorption spectrometer (Beijing Puxi General Instruments Co., Ltd, Beijing, China). A series of corresponding metal standard solutions were used to determine the standard curve. The sample was diluted with deionized water and the absorbance was determined by flame method, then the metal concentration was obtained by standard curve.

### 3. Results and Discussion

#### 3.1. Gold Dissolving Effect of $\text{CHI}_3/\text{BmimN}(\text{CN})_2$

The clear and golden yellow solution after dissolving indicates that the  $\text{CHI}_3/\text{BmimN}(\text{CN})_2$  composite solution has a good solubility for  $\text{Au}^0$  (13 W incandescent lamp, 25 °C,  $\text{BmimN}(\text{CN})_2 = 3$  g,  $\text{CHI}_3 = 0.5$  g, gold = 0.006 g) (Figure 1). The result of AAS shows that the leaching yield of gold is 100 wt% under 13 W incandescent light at room temperature (Table 1).



**Figure 1.** Gold dissolved in  $\text{CHI}_3/\text{BmimN}(\text{CN})_2$  under light condition.

**Table 1.** Gold leaching yield with different reagents and conditions.

Reagent	Illuminant	Leaching Yield/wt%
$\text{BmimN}(\text{CN})_2$	No additional illuminant	0
$\text{CHI}_3$	No additional illuminant	0
$\text{BmimN}(\text{CN})_2 + \text{CHI}_3$	No additional illuminant	0
$\text{BmimN}(\text{CN})_2$	13 W incandescent lamp	0
$\text{CHI}_3$	13 W incandescent lamp	6.8
$\text{BmimN}(\text{CN})_2 + \text{CHI}_3$	13 W incandescent lamp	100

Reaction conditions: 25 °C, 5h,  $\text{BmimN}(\text{CN})_2 = 3$  g,  $\text{CHI}_3 = 0.5$  g, gold = 0.006 g.

To verify the key factors of gold dissolution in this system, comparative experiments were carried out. The results are shown in Table 1: With light, the gold dissolution yield was 0 wt% by  $\text{BmimN}(\text{CN})_2$  alone and only 6.8 wt% by  $\text{CHI}_3$  alone, but could reach 100 wt% by  $\text{CHI}_3/\text{BmimN}(\text{CN})_2$ ; without light, the gold dissolution yield remained at 0 wt% by all three solutions. Therefore, it is expected that  $\text{BmimN}(\text{CN})_2$  and  $\text{CHI}_3$  play a synergistic role in the process of gold dissolution, and light is the key factor to initiate the reaction.

In addition, the effect of the ratio of  $\text{CHI}_3$  and  $\text{Au}^0$  on the reaction rate was investigated. Under the condition of light, 3 g  $\text{BmimN}(\text{CN})_2$  was mixed with different amount of  $\text{CHI}_3$  and added to 0.006 g  $\text{Au}^0$ . The average dissolution rate of gold was detected by AAS after stirring for 3 h. As shown in Figure 2, the dissolution rate of  $\text{Au}^0$  gradually increases with the increase of  $\text{CHI}_3$ . When the mass ratio of  $\text{CHI}_3$  to  $\text{Au}^0$  is 100:6, 200:6, 300:6, 500:6, and 1000:6, the average dissolution rates are 0.018 mg/min and 0.046 mg/min, 0.103 mg/min,

0.242 mg/min, and 0.282 mg/min, respectively. There is a rapid rise in the dissolution rate with the increase of  $\text{CHI}_3$  before 500:6 ( $\text{CHI}_3$  to  $\text{Au}^0$ ) mass ratio, but only a slight increase after 500:6 ratio. Therefore, considering the economic and efficiency factors, the suitable ratio of  $\text{CHI}_3$  to  $\text{Au}^0$  is 500:6.

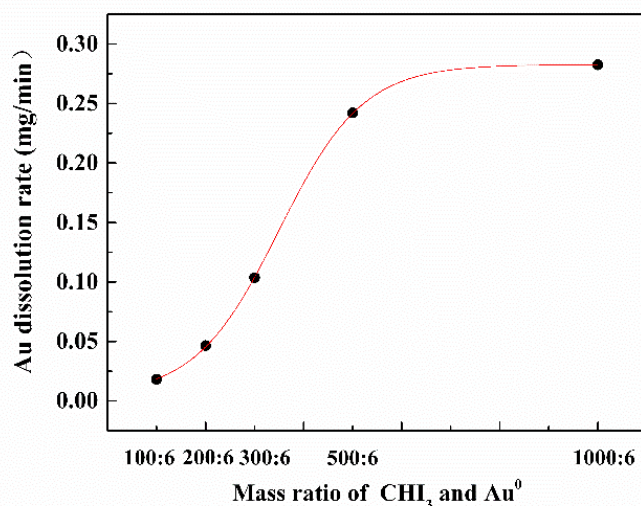


**Figure 2.** Variation of dissolution rate with ratio of  $\text{CHI}_3$  and  $\text{Au}^0$ .

With the optimal ratio ( $\text{CHI}_3 = 0.5$  g,  $\text{BmimN}(\text{CN})_2 = 3$  g,  $\text{Au} = 0.006$  g), the average gold dissolution rate in 5 h is  $945 \text{ mg Au}/(\text{h}\cdot\text{mol}\cdot\text{CHI}_3)$  under light condition, and the leaching yield variation with time is shown in Table S1. Compared with other methods [26] (Table 2), it is clear that  $\text{CHI}_3/\text{BmimN}(\text{CN})_2$  has the fastest gold dissolution rate, which is 18.9 times higher than that of the cyanidation method.

**Table 2.** Comparison of gold dissolution rate with other methods in literature [26].

Reagent or Mixtures	Condition	Dissolution Rate
$\text{CHI}_3$ 0.42 M, $\text{BmimN}(\text{CN})_2$ 4.87 M	$25^\circ\text{C}/13\text{W}$ incandescent light	$945 \text{ mg Au}/(\text{h}\cdot\text{mol}\cdot\text{CHI}_3)$
$(\text{NH}_4)_2\text{S}_2\text{O}_3$ 0.3 M, $\text{NH}_3$ 0.3 M, $\text{CuSO}_4$ 0.01 M	$25^\circ\text{C}$	$13.3 \text{ mg Au}/(\text{h}\cdot\text{mol}\cdot(\text{NH}_4)_2\text{S}_2\text{O}_3)$
$\text{CH}_4\text{N}_2\text{S}$ 0.263 M, $\text{Fe}_2(\text{SO}_4)_3$ 0.02 M, $\text{H}_2\text{SO}_4$ 0.15 M	$25^\circ\text{C}$	$13.3 \text{ mg Au}/(\text{h}\cdot\text{mol}\cdot\text{CH}_4\text{N}_2\text{S})$
Aqua Regia ( $\text{HNO}_3$ 1.74 M, $\text{HCl}$ 8.92 M)	$25^\circ\text{C}$	$82.2 \text{ mg Au}/(\text{h}\cdot\text{mol}\cdot\text{HNO}_3)$
$\text{KCN}$ 0.14 M	$25^\circ\text{C}$	$50 \text{ mg Au}/(\text{h}\cdot\text{mol}\cdot\text{KCN})$

### 3.2. Reaction Mechanism

To verify the effect of gold in the process of gold dissolution in the complex ionic liquid system, a gold-free contrast experiment was performed (Figure 3). Under the same light condition, the sample without gold turns blue after adding the starch solution, indicating the presence of  $\text{I}_2$  in the process. However, the sample with gold is yellow after dissolving, and does not turn blue when mixed with the starch solution, indicating the absence of  $\text{I}_2$  in the solution after reaction. The possible reason is that  $\text{CHI}_3$  produces iodine free radicals under light condition. In the absence of gold, iodine free radicals are combined to form iodine. In the presence of gold, the iodine free radicals can strip the electrons from the gold and oxidize the gold.

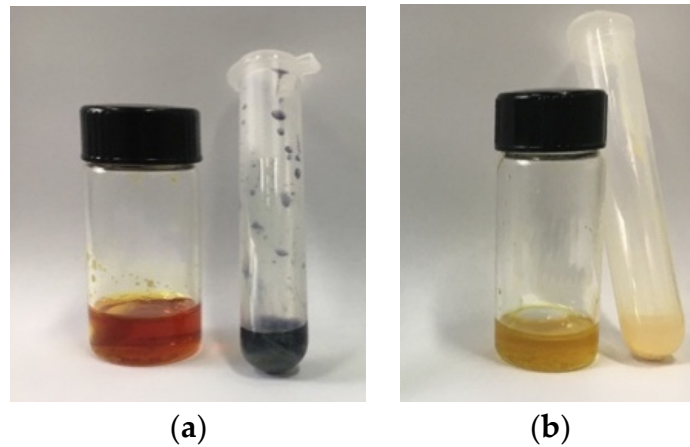
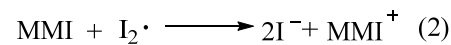
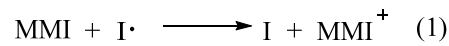


**Figure 3.** Mixing of ionic liquid system and starch solution: (a) without Au<sup>0</sup>, (b) with Au<sup>0</sup>.

Thiamazole (MMI) is an inhibitor of iodine free radicals [27]. It reacts with iodine free radicals as Scheme 1 to inhibit the oxidation of free radicals, and it will not affect the coordination of ionic liquids.



**Scheme 1.** Reaction of MMI with iodine free radical.

After adding different proportions of MMI in CHI<sub>3</sub>/BmimN(CN)<sub>2</sub> under the same conditions, the results are shown in Figure 4. With the increasing of the molar ratio of MMI to CHI<sub>3</sub>, the leaching yield decreased significantly. When the molar ratio is greater than 3, the gold was no longer dissolved. The results further confirm that the iodine free radical is the oxidation species in the leaching process.

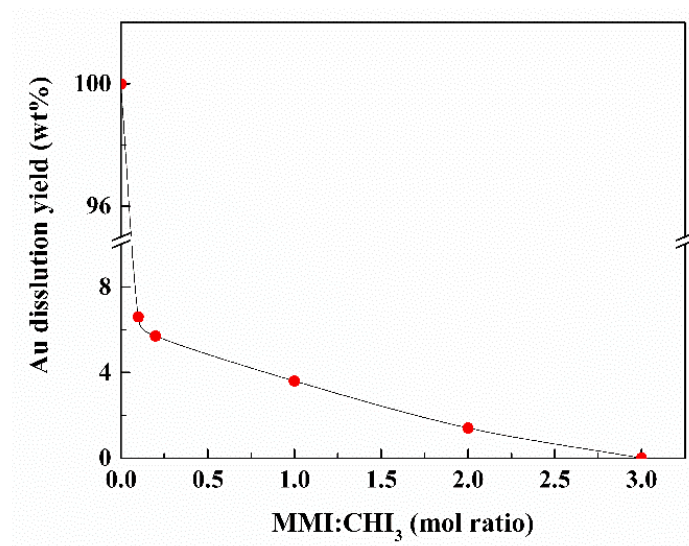


**Figure 4.** Effect of MMI on leaching yield of gold.

It was found that some crystals were precipitated at room temperature from the ionic liquid solution after gold leaching (Figure 5a). The SXRDR result (Table S2) shows that the crystal structure (Figure 5b) is 1-butyl-3-methylimidazolium iodide (BmimI) with no gold presented, which indicates that the leached gold remains stably in the solution and does not precipitate over time.

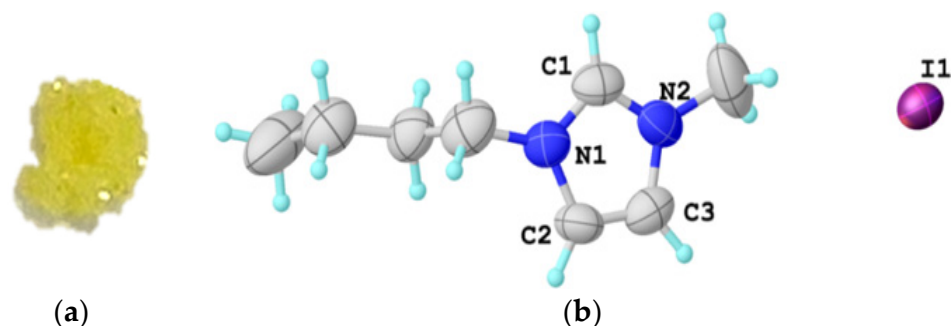


Figure 5. (a) Crystal precipitated after reaction; (b) composition of crystal.

The UV-Vis results are shown in Figure 6 and the sample shows absorption peaks at 227 nm, 273 nm, and 340 nm after the gold is dissolved. The absorption peak of  $\text{Au}^0$  is above 500 nm [28], so the Au in the sample after dissolution does not exist as a dispersed zero-valent gold colloid, but a high-valent gold ion. The absorption peak of Au(I) complexes is usually in the range of 200 nm–470 nm [29]. The sample absorption peaks at 227 nm and 273 nm are similar to  $(n\text{-BuNC})\text{AuICN}$  [30]. Therefore, it can be inferred that the dissolved gold exists in the form of monovalent gold. In addition, the absorption peak at 340 nm belongs to the remaining  $\text{CHI}_3$ .

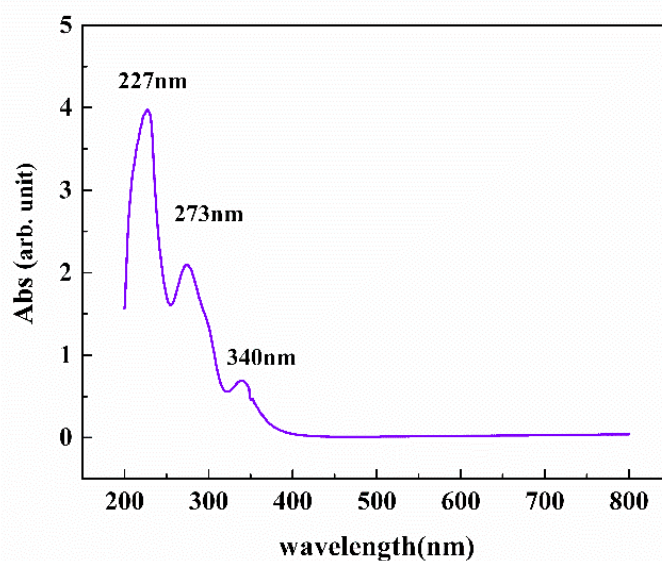


Figure 6. UV-Vis spectrum of  $\text{Au}^0$  dissolved in ionic liquid system.

To further explore the valence and structure of Au after dissolving in the ionic liquid system, XPS tests were performed on the dissolved gold products obtained. From the results shown in Figure 7, the Au  $4f_{7/2}$  orbital binding energy is 85.2 eV. Combined with the study of Vernon et al. [31], it is attributed to the Au(I) in the  $[\text{Bmim}][\text{Au}(\text{N}(\text{CN})_2)_2]$  ion pair formed by the coordination of  $\text{BmimN}(\text{CN})_2$  and  $\text{AuN}(\text{CN})_2$ . The characteristic binding energy of Au(I) in Au I is 84.4 eV [32], so Au I does not exist in the solution. The binding energy of I  $3d_{5/2}$  orbital is 618.2 eV. Combined with the SXRD results, it is expected that it belongs to  $\text{I}^-$  bound to  $\text{Bmim}^+$ . According to the research of Solymosi et al. [33], the peak at 619.1 eV is attributed to the I of  $\text{CHI}_3$ .

According to the XPS results, in the ionic liquid system after leaching, gold exists in the form of  $[\text{Bmim}][\text{Au}(\text{N}(\text{CN})_2)_2]$  ion pairs, and iodide ions are combined with imidazole cations. Moreover,  $\text{CHI}_3$  still exists in the system after the reaction, which is consistent with the UV-Vis results.

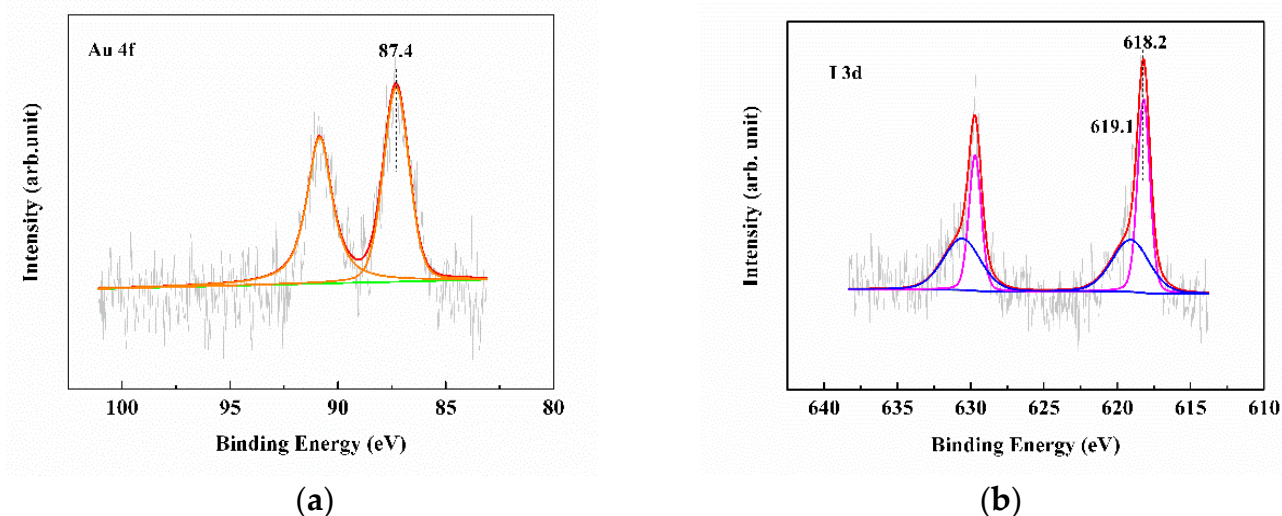
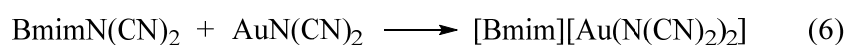
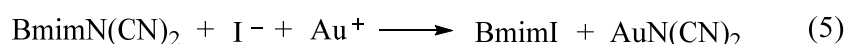
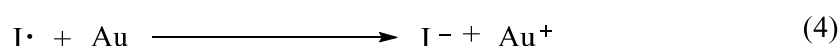
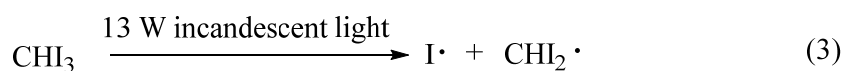


Figure 7. XPS spectrum of Au<sup>0</sup> dissolved in ionic liquid system under lighting condition: (a) Au 4f, (b) I 3d.

Combining the above characterization and analysis results, the possible reaction mechanism is shown in Scheme 2 and Figure 8: Light induces the formation of iodine free radicals in CHI<sub>3</sub> (step (3)), then I captures the electrons on Au<sup>0</sup> to form Au<sup>+</sup> (step (4)), which then combines with N(CN)<sub>2</sub><sup>−</sup> to form AuN(CN)<sub>2</sub> (step (5)). Subsequently, the imidazole cation of the ionic liquid forms a stable [Bmim]·[AuN(CN)<sub>2</sub>]<sub>2</sub> ion pair through various intermolecular forces such as electrostatic attraction, hydrogen bonding, and cation-π bonding with AuN(CN)<sub>2</sub> [34–36] (step (6)). The ion-pair structure makes the metal shed from the particle surface exist in the ionic liquid in a stable form, and shifts the balance of the oxidation (step (4)) to the right, which further promotes the dissolution reaction and finally promotes the continuous dissolving of the gold particles into the ionic liquid system. In addition, the new ionic liquid BmimI obtained by ion exchange is partially precipitated in the form of crystals.



Scheme 2. Mechanism of dissolution of gold by CHI<sub>3</sub>/BmimN(CN)<sub>2</sub>.

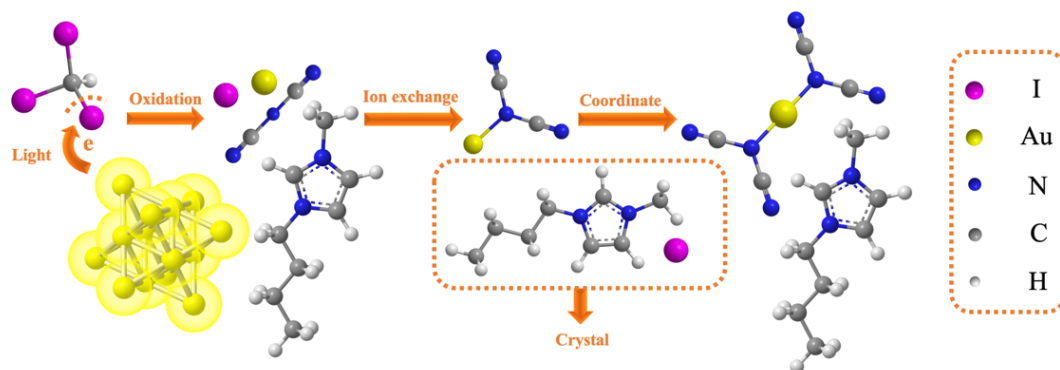


Figure 8. Reaction mechanism diagram.

#### 4. Application of Precious Metal Extraction Method

In the actual recycling process, the existing form of gold would be more complex. To further evaluate the potential of the new method in practical application, the extraction efficiency of gold ore, WEEE, and spent catalysts was evaluated.

##### 4.1. Extraction Gold from Ore

The gold ore used is shown in Figure S1, and its XRF spectroscopy result (Table S3) indicates that a variety of metal elements are present in the gold ores, including gold (0.0244 wt%), iron (2.07 wt%), and copper (0.413 wt%). The maximum gold leaching yield under light condition obtained using the  $\text{CHI}_3/\text{BmimN}(\text{CN})_2$  leaching system is approximately 81.9 wt%. However, the leaching yield for iron and copper is only 7.5 wt% and 15.4 wt%, respectively, so the system can effectively leach gold from the ore with complex composition in actual situation.

##### 4.2. Extraction Gold from WEEE

As illustrated in Figure S2, the metal pins on the CPU chip are cut off before leaching. At 25 °C, 0.01 g CPU pins can be completely dissolved by  $\text{BmimN}(\text{CN})_2$  and 0.5 g  $\text{CHI}_3$  under light condition within 5 h, the leaching yields of Au and Cu are both 100 wt% as revealed by AAS results.

##### 4.3. Extraction Gold from Spent Catalyst

The  $\text{Au@SiO}_2$  catalyst used is shown in Figure S3. According to XRF analysis, the gold content of the catalyst is 0.381 wt% (Table S4). One gram of  $\text{Au@SiO}_2$  catalyst was added to 3 g  $\text{BmimN}(\text{CN})_2$  and 0.5 g  $\text{CHI}_3$ , and stirred at 25 °C for 5 h under 13 W incandescent light. Then the catalyst was separated and extracted by Soxhlet extraction with 150 mL acetone at 100 °C for 24 h. The results of AAS showed the leaching yield of gold was 64.9 wt% before Soxhlet extraction and 100 wt% after Soxhlet extraction.

The results of XRF analysis (Table S5) show that the residual amount of gold in the catalyst before and after Soxhlet extraction is 0.136 wt% and 0 wt%, respectively, which is consistent with the results of AAS. It also shows that the extraction yield of gold is 100 wt% after Soxhlet extraction.

In addition, the catalyst carrier before leaching and the catalyst carrier after leaching (before and after Soxhlet extraction) were characterized by XRD. It can be seen from Figure 9 that the XRD diffraction peaks before leaching are at  $2\theta = 38^\circ, 44^\circ, 64^\circ,$  and  $77^\circ$ , which correspond to  $\text{Au}^0$ 's (1 1 1), (2 0 0), (2 2 0), and (3 1 1) crystal planes. As the substrate used in the XRD test is  $\text{SiO}_2$ , the diffraction peak at  $2\theta = 10^\circ\text{--}30^\circ$  is attributed to amorphous  $\text{SiO}_2$ . In the XRD result before Soxhlet extraction, the diffraction peaks at  $13^\circ$  and  $26^\circ$  belong to  $\text{BmimI}$  crystal [37]. There is no diffraction peak of  $\text{Au}^0$  in the sample after leaching, indicating that  $\text{Au}^0$  has all been oxidized to gold ions and loaded in the ionic liquid phase. However, the carrier has a certain adsorption effect on ionic liquids due to its large surface area, so a small part of ionic liquids and gold ions are adsorbed on the carrier surface.

To further explore the valence state of Au in the catalyst after dissolving in the ionic liquid system, XPS tests were performed on the catalyst at different operating stages, and the results are shown in Figure 10. The binding energies of the Au  $4f_{7/2}$  orbital before leaching and after leaching (before Soxhlet extraction) are 83.7 eV (belongs to  $\text{Au}^0$ ) [38] and 85.2 eV (belongs to  $[\text{Bmim}]\cdot[\text{Au}(\text{N}(\text{CN})_2)_2]$ ) [31], respectively, while there is no Au peak in the carrier after Soxhlet extraction.

In general, the extraction of gold from the catalyst requires two steps. In the first step of leaching process, gold is oxidized to Au(I) and then coordinated with ionic liquid to form  $[\text{Bmim}]\cdot[\text{Au}(\text{N}(\text{CN})_2)_2]$  ion pair, which be partly absorbed by the carrier. The subsequent Soxhlet extraction process can remove all the gold ions from the catalyst surface.

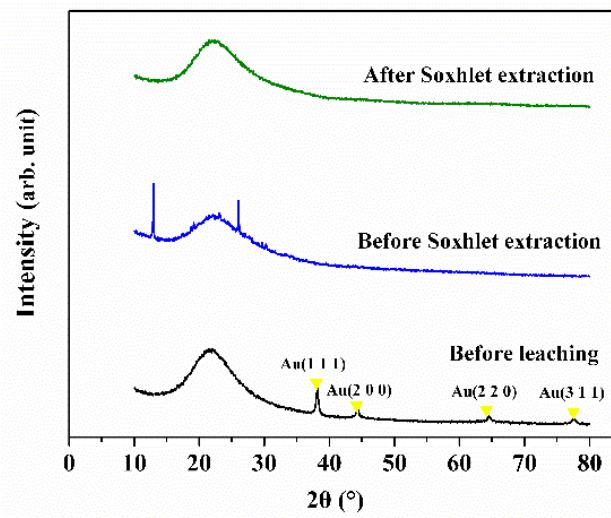


Figure 9. XRD spectra of catalysts in different stages.

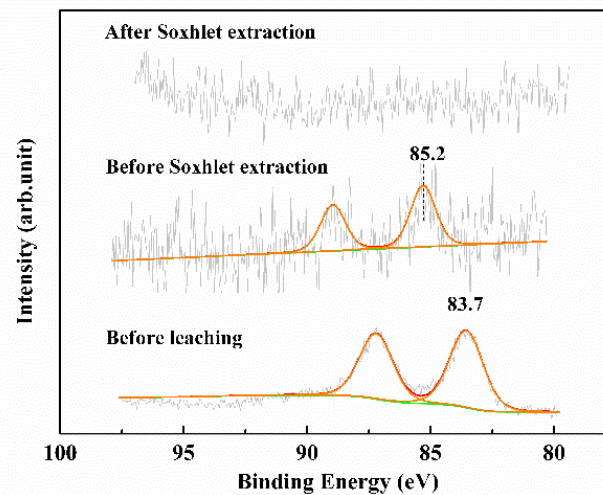


Figure 10. XPS spectra of catalysts in different stages.

## 5. Conclusions

In this study, 100 wt% gold leaching yield has been achieved by using  $\text{CHI}_3$  and  $\text{BmimN}(\text{CN})_2$  composite ionic liquid under  $25^\circ\text{C}$  and light condition. The average dissolution rate of gold is  $945 \text{ mgAu}/(\text{h}\cdot\text{mol}\cdot\text{CHI}_3)$ , which is 18.9 times of that of the traditional cyanidation method. Under the synergistic effect of the oxidation ability of iodine free radical and the coordination ability of ionic liquid, gold can form a more stable complex with ionic liquid after losing electrons to promote the oxidation process, which provides a new gold-leaching method. Moreover, the application of this method has been further studied in the recovery of precious metals from ores, WEEE, and spent catalysts. Compared with traditional recovery methods, this method is more efficient, simple, and environmentally friendly and shows significant adaptability for practical applications.

**Supplementary Materials:** The following are available online at <https://www.mdpi.com/article/10.3390/met11060919/s1>. Figure S1: The gold ores utilized for the gold leaching, Figure S2: The waste CPU pins utilized for the gold leaching, Figure S3: The  $\text{Au@SiO}_2$  catalyst utilized for the gold leaching, Table S1: The leaching yield variation of time, Table S2: SXRD result of the crystal, Table S3: XRF results of gold ore, Table S4: XRF result of gold catalyst, Table S5: XRF results of catalyst before and after Soxhlet extraction.

**Author Contributions:** Conceptualization, F.F.; methodology, J.L.; validation, L.Y. and J.L.; formal analysis, C.L.; investigation, M.Z.; resources, X.L.; data curation, Q.Z.; writing—original draft preparation, Y.S.; writing—review and editing, F.F. and J.C.; visualization, H.W.; supervision, J.Z.; project administration, X.L.; funding acquisition, F.F. All authors have read and agreed to the published version of the manuscript.

**Funding:** This research was funded by the National Natural Science Foundation of China, grant number 22078302,21978265,22078292,21776258.

**Institutional Review Board Statement:** Not applicable.

**Informed Consent Statement:** Not applicable.

**Data Availability Statement:** The data used in this article are presented in the manuscript.

**Conflicts of Interest:** The authors declare no conflict of interest.

## References

1. Das, N. Recovery of precious metals through biosorption—A review. *Hydrometallurgy* **2010**, *103*, 180–189. [[CrossRef](#)]
2. Syed, S. Recovery of gold from secondary sources-A review. *Hydrometallurgy* **2012**, *115–116*, 30–51. [[CrossRef](#)]
3. Bond, G.C.; Thompson, D.T. Catalysis by Gold. *Catal. Rev. Sci. Eng.* **1999**, *41*, 319–388. [[CrossRef](#)]
4. Haruta, M.; Daté, M. Advances in the catalysis of Au nanoparticles. *Appl. Catal. A Gen.* **2001**, *222*, 427–437. [[CrossRef](#)]
5. Choudhary, T.V.; Goodman, D.W. Oxidation catalysis by supported gold nano-clusters. *Top. Catal.* **2002**, *21*, 25–34. [[CrossRef](#)]
6. Hashmi, A.S.K.; Hutchings, G.J. Gold Catalysis. *Angew. Chem. Int. Ed.* **2006**, *45*, 7896–7936. [[CrossRef](#)] [[PubMed](#)]
7. Kung, M.C.; Davis, R.J.; Kung, H.H. Understanding Au-Catalyzed Low-Temperature CO Oxidation. *J. Phys. Chem. C* **2007**, *111*, 11767–11775. [[CrossRef](#)]
8. Pina, C.D.; Falletta, E.; Prati, L.; Rossi, M. Selective oxidation using gold. *Chem. Soc. Rev.* **2008**, *37*, 2077–2095. [[CrossRef](#)]
9. Corma, A.; Garci, H. Supported gold nanoparticles as catalysts for organic reactions. *Chem. Soc. Rev.* **2008**, *37*, 2096–2126. [[CrossRef](#)] [[PubMed](#)]
10. Wu, H.; Pantaleo, G.; Venezia, A.M.; Liotta, L.F. Mesoporous silica based gold catalysts: Novel synthesis and application in catalytic oxidation of CO and volatile organic compounds (VOCs). *Catalysts* **2013**, *3*, 774–793. [[CrossRef](#)]
11. Kakumazaki, J.; Kato, T.; Sugawara, K. Recovery of gold from incinerated sewage sludge ash by chlorination. *ACS Sustain. Chem. Eng.* **2014**, *2*, 2297–2300. [[CrossRef](#)]
12. Dorin, R.; Woods, R. Determination of leaching rates of precious metals by electrochemical techniques. *J. Appl. Electrochem.* **1991**, *21*, 419–424. [[CrossRef](#)]
13. Hilson, G.; Monhemius, A.J. Alternatives to cyanide in the gold mining industry: What prospects for the future? *J. Clean. Prod.* **2006**, *14*, 1158–1167. [[CrossRef](#)]
14. Altansukh, B.; Haga, K.; Ariunbolor, N.; Kawamura, S. Leaching and Adsorption of Gold from Waste Printed Circuit Boards Using Iodine-Iodide Solution and Activated Carbon. *Eng. J.* **2016**, *20*, 29–40. [[CrossRef](#)]
15. Birloaga, I.; De Michelis, I.; Ferella, F.; Buzatu, M.; Vegliò, F. Study on the influence of various factors in the hydrometallurgical processing of waste printed circuit boards for copper and gold recovery. *Waste Manag.* **2013**, *33*, 935–941. [[CrossRef](#)] [[PubMed](#)]
16. Jingying, L.; Xiuli, X.; Wenquan, L. Thiourea leaching gold and silver from the printed circuit boards of waste mobile phones. *Waste Manag.* **2012**, *32*, 1209–1212. [[CrossRef](#)]
17. Sahin, M.; Akcil, A.; Erust, C.; Altynbek, S.; Gahan, C.S.; Tuncuk, A. A Potential Alternative for Precious Metal Recovery from E-waste: Iodine Leaching A Potential Alternative for Precious Metal Recovery from E-waste: Iodine Leaching. *Sep. Sci. Technol.* **2015**, *50*, 2587–2595.
18. Ha, V.H.; Lee, J.; Huynh, T.H.; Jeong, J.; Pandey, B.D. Optimizing the thiosulphate leaching of gold from printed circuit boards of discarded mobile phone. *Hydrometallurgy* **2014**, *149*, 118–126. [[CrossRef](#)]
19. Marsh, K.N.; Boxall, J.A.; Lichtenthaler, R. Room temperature ionic liquids and their mixtures—A review. *Fluid Phase Equilib.* **2004**, *219*, 93–98. [[CrossRef](#)]
20. Visser, A.E.; Swatloski, R.P.; Reichert, W.M.; Mayton, R.; Sheff, S.; Wierzbicki, A.; Davis, J.; Rogers, R.D. Task-specific ionic liquids for the extraction of metal ions from aqueous solutions. *Chem. Commun.* **2001**, *1*, 135–136. [[CrossRef](#)]
21. Ashkenani, H.; Taher, M.A. Use of ionic liquid in simultaneous microextraction procedure for determination of gold and silver by ETAAS. *Microchem. J.* **2012**, *103*, 185–190. [[CrossRef](#)]
22. Egorov, V.M.; Djigailo, D.I.; Momotenko, D.S.; Chernyshov, D.V.; Torocheshnikova, I.I.; Smirnova, S.V.; Pletnev, I.V. Task-specific ionic liquid trioctylmethylammonium salicylate as extraction solvent for transition metal ions. *Talanta* **2010**, *80*, 1177–1182. [[CrossRef](#)] [[PubMed](#)]
23. Vázquez-Zavala, A.; García-Gómez, J.; Gómez-Cortés, A. Study of the structure and selectivity of Pt-Au catalysts supported on Al<sub>2</sub>O<sub>3</sub>, TiO<sub>2</sub>, and SiO<sub>2</sub>. *Appl. Surf. Sci.* **2000**, *167*, 177–183. [[CrossRef](#)]
24. Lund, C.; Lamberg, P.; Lindberg, T. Practical way to quantify minerals from chemical assays at Malmberget iron ore operations—An important tool for the geometallurgical program. *Miner. Eng.* **2013**, *49*, 7–16. [[CrossRef](#)]

25. Gallas-Hulin, A.; Kotni, R.K.; Nielsen, M.; Kegnaes, S. Catalytic Oxidation of Allylic Alcohols to Methyl Esters. *Top. Catal.* **2017**, *60*, 1380–1386. [[CrossRef](#)]
26. Birich, A.; Stopic, S.; Friedrich, B. Kinetic Investigation and Dissolution Behavior of Cyanide Alternative Gold Leaching Reagents. *Sci. Rep.* **2019**, *9*, 1–10. [[CrossRef](#)] [[PubMed](#)]
27. Taylor, J.J.; Willson, R.L.; Kendall-Taylor, P. Evidence for direct interactions between methimazole and free radicals. *FEBS Lett.* **1984**, *176*, 337–340. [[CrossRef](#)]
28. System, M.; Paclawski, K.; Jaworski, W.; Streszewski, B.; Fitzner, K. Trends in Colloid and Interface Science XXIV. *Prog. Colloid Polym. Sci.* **2011**, *138*, 39–44.
29. Rawashdeh-Omary, M.A.; Omary, M.A.; Patterson, H.H. Oligomerization of  $\text{Au}(\text{CN})_2^-$  and  $\text{Ag}(\text{CN})_2^-$  ions in solution via ground-state aurophilic and argentophilic bonding. *J. Am. Chem. Soc.* **2000**, *122*, 10371–10380. [[CrossRef](#)]
30. White-Morris, R.L.; Stender, M.; Tinti, D.S.; Balch, A.L.; Rios, D.; Attar, S. New Structural Motifs in the Aggregation of Neutral Gold(I) Complexes: Structures and Luminescence from (Alkyl isocyanide)AuCN. *Inorg. Chem.* **2003**, *42*, 3237–3244. [[CrossRef](#)]
31. Vernon, C.F.; Fawell, P.D.; Klauber, C. XPS investigation of the states of adsorption of aurocyanide onto crosslinked polydiallylamine and commercial anionexchange resins. *React. Polym.* **1992**, *18*, 35–45. [[CrossRef](#)]
32. Kitagawa, H.; Kojima, N.; Nakajima, T. Studies of Mixed-valence States in Three-dimensional Halogen-bridged Gold Compounds,  $\text{Cs}_2\text{Au}_1\text{AU}_{\text{III}}\text{X}$ , (X = Cl, Br or I). Part 2. X-Ray Photoelectron Spectroscopic Study. *J. Chem. Soc. Dalton Trans.* **1991**, *2*, 3121–3125. [[CrossRef](#)]
33. Solymosi, F.; Kovács, I. Carbon-carbon coupling of methylene groups: Thermal and photo-induced dissociation of  $\text{CH}_2\text{I}_2$  on Pd(100) surface. *Surf. Sci.* **1993**, *296*, 171–185. [[CrossRef](#)]
34. Mota, A.; Hallett, J.P.; Kuznetsov, M.L.; Correia, I. Structural characterization and DFT study of VIVO(acac) 2 in imidazolium ionic liquids. *Phys. Chem. Chem. Phys.* **2011**, *13*, 15094–15102. [[CrossRef](#)] [[PubMed](#)]
35. Xu, Z.X.; Zhao, Y.L.; Liang, W.Y.; Zhou, P.P.; Yang, Y. A novel: N-methylimidazolium-based poly(ionic liquid) to recover trace tetrachloroaurate from aqueous solution based on multiple supramolecular interactions. *Inorg. Chem. Front.* **2018**, *5*, 922–931. [[CrossRef](#)]
36. Maton, C.; Brooks, N.R.; Van Meervelt, L.; Binnemans, K.; Schaltin, S.; Fransaer, J.; Stevens, C.V. Synthesis and properties of alkoxy- and alkenyl-substituted peralkylated imidazolium ionic liquids. *ChemPhysChem* **2013**, *14*, 3503–3516. [[CrossRef](#)]
37. Farhana, N.K.; Khanmirzaei, M.H.; Omar, F.S.; Ramesh, S.; Ramesh, K. Ionic conductivity improvement in poly (propylene) carbonate-based gel polymer electrolytes using 1-butyl-3-methylimidazolium iodide (BmimI) ionic liquid for dye-sensitized solar cell application. *Ionics* **2017**, *23*, 1601–1605. [[CrossRef](#)]
38. Seah, M.P.; Gilmore, I.S.; Beamson, G. XPS: Binding energy calibration of electron spectrometers 5-Re-evaluation of the reference energies. *Surf. Interface Anal.* **1998**, *26*, 642–649. [[CrossRef](#)]